

⁹Dimensions: $F = \text{erg}$; $A, f, \Delta f = \text{erg cm}^{-3}$; $C = \text{g cm}^{-3}$; $\mu = \text{erg cm}^{-1}$; $\vec{J} = \text{g cm}^{-2} \text{sec}^{-1}$; $M = \text{g}^2 \text{erg}^{-1} \text{cm}^{-1} \text{sec}^{-1}$; $\kappa = \text{erg cm}^3 \text{g}^{-2}$; $m = \text{g mole}^{-1}$.

¹⁰J. E. Hilliard, *Phase Transformations* (American Society for Metals, Metals Park, Ohio, 1970).

¹¹L. D. Landau and E. M. Lifshitz, *Fluid Mechanics* (Addison-Wesley, Reading, Mass., 1959), Chap. 6.

¹²C. Warren and W. W. Webb, *J. Chem. Phys.* **50**, 3694 (1969).

¹³H. Brenner, *Prog. Heat Mass Transfer* **5**, 89 (1972).

Binding Energies for Different Adsorption Sites of Hydrogen on Simple Metals*

O. Gunnarsson† and H. Hjelmberg

Institute of Theoretical Physics, Chalmers University of Technology, Fack, S-402 20 Göteborg 5, Sweden

and

B. I. Lundqvist

Institute of Physics, University of Aarhus, DK-8000 Århus C, Denmark

(Received 9 February 1976)

A self-consistent calculation for hydrogen chemisorption is reported, where the surface is described both by the jellium model and by a model that includes ion pseudopotentials to lowest order. It predicts that for H on Al(100) a bridge configuration is the most favorable (binding energy 1.9 eV), and that the activation energy for surface diffusion is 0.1–0.2 eV.

This note reports the first results of a calculation with a formalism that in principle applies quite generally for chemisorption on a real substrate. We compute the dependence of the binding energy of an adatom on the separation from the surface and on the surface geometry. In the case of hydrogen on Al(100), our model predicts atomic adsorption in a bridge position at low temperatures, the activation energy for surface diffusion being 0.1–0.2 eV. The binding results from a gain in potential energy due to the contraction of charge around the proton, the consequent increase in kinetic energy being partially balanced by the reduction due to the substantial mixing of adatom and substrate states.

Figure 1 shows results obtained using parameters for the above system. For a hydrogen atom on a semi-infinite jellium, our results are in general agreement with those recently published by Lang and Williams (LW).¹ The energy curves of Fig. 1 for H on an Al(100) surface are calculated by lowest-order perturbation theory with an array of pseudopotentials² representing the lattice. Our scheme predicts that the bridge position provides the highest binding energy, namely 1.9 eV (cf. 3.0 eV for the Al-H molecule³). As the dissociation energy of the H₂ molecule is 2.4 eV per atom (excluding the vibrational component), this implies that on this Al surface there would be no dissociative adsorption, in apparent agreement with experiment.⁴

The diffusion of an H atom along the surface is predicted to occur from one bridge position to another at a distance of 1.6–1.9 Å from the nearest Al atom, with an activation energy of 0.1–0.2 eV. An Arrhenius law with a prefactor of 10¹³ sec⁻¹ suggests temperatures below 30–50 K to prevent recombination and molecular desorption.⁵

The distances between the proton and the near-

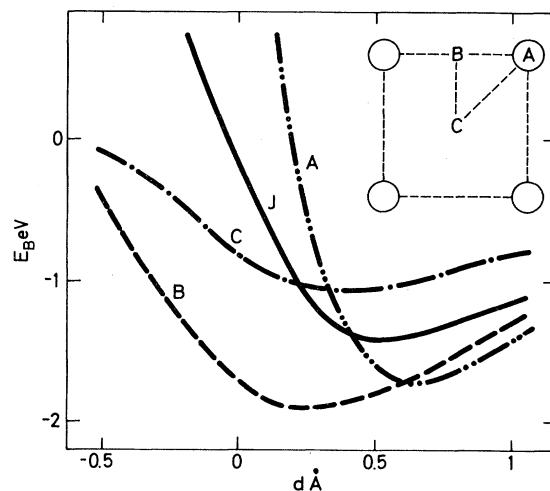


FIG. 1. Calculated energy curves for hydrogen chemisorbed on jellium (J , $r_s=2$) and in atop (A), bridge (B), and centered (C) positions on a (100) surface of Al. The distance between the H atom and the jellium edge is denoted d . The inset is a figure of the unit cell of the Al(100) surface, defining the A , B , and C positions.

est Al atom, $d_{\text{Al-H}} = 1.9 \text{ \AA}$ for the equilibrium bridge position and $d_{\text{Al-H}} = 1.6 \text{ \AA}$ for the atop position, correlate well with the distance 1.65 \AA for the Al-H molecule.³ Geometrical restrictions make such short distances unattainable in the more symmetric, centered position. Important factors determining these bond lengths are the strong repulsion when the H atom attempts to penetrate the ion cores of the substrate, and the rapid increase in kinetic energy when the adatom goes into the surface. For instance, by moving the proton from $z = 1$ to -0.5 \AA , the kinetic energy (calculated in the jellium model) increases by almost 10 eV owing to the reduced volume available for the electrons. Because of the interaction with the ion cores, the repulsive part of the energy curve for the atop position is very similar to the corresponding curve³ for the Al-H molecule. In this position it is found to be energetically unfavorable for the adatom charge to penetrate the substrate cores. This would occur for $d_{\text{Al-H}} < r_c + r_H$, where r_c is the core radius of the pseudopotential² and r_H ($\sim 1 \text{ \AA}$) is the radius of the sphere around the proton containing one electron. Using the distance $r_c + r_H$ as an estimate of the atop equilibrium position for H on free-electron-like substrates such as Al, Mg, Na, K, Rb, and Cs gives ion-proton separations which agree within 5% with the bond lengths of the corresponding hydride molecules.⁶

Some features of the adatom-metal bond can be illustrated by the adatom-induced density $\Delta\rho(\vec{r})$ as calculated for H on semi-infinite jellium. Figure 2 shows how, at the equilibrium distance (0.6 \AA outside the background-charge edge at $r_s = 2$), the adatom charge is contracted compared with the free atom. This contractive promotion⁷ is the prime source of the binding, the nuclear attraction of the adatom electron charge increasing from -27 to -31 eV . The associated increase in kinetic energy is partially balanced by a reduction due to the smoothing of the wave functions for low-lying bonding-type levels, associated with the sharing of the electrons.⁷ The adatom density of states¹⁸ shows a behavior typical of weak chemisorption with one atomic resonance.⁹ Contrary to popular belief, the one-electron potential does not show a barrier between adatom and substrate. Nevertheless the width of the H(1s) resonance is relatively small. This may be understood within an Anderson-model⁹ context, if one notes that the hopping matrix elements should be reduced considerably when the over-completeness and nonorthogonality of the basis

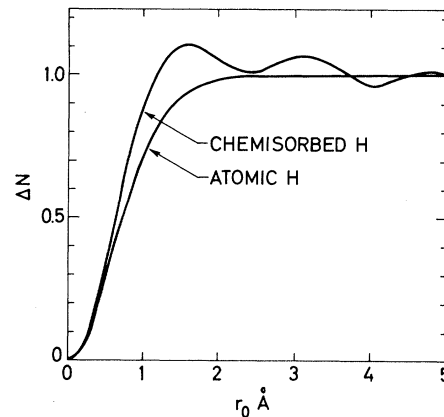


FIG. 2. The adatom-induced electron density $\Delta\rho(\vec{r})$ compared with the density of atomic hydrogen, plotted as the amount of electronic charge within a sphere of radius r_0 , $\Delta N(r_0) = \int_0^{r_0} r^2 dr d\Omega \Delta\rho(\vec{r})$.

functions are taken into account.

The charge which is built up around the proton and along the bond is taken primarily from the metal region close to the adatom. The charge transfer is small, however, with roughly 0.1 electron displaced across the surface. That this is a case of neutral chemisorption is further illustrated by the electrostatic adatom-metal interaction being very small. Figure 2 shows some solid-state aspects of the chemisorption: the rapid screening of the perturbation and the associated Friedel oscillations.

The method¹⁰ we use for chemisorption calculations describes the low-coverage limit, includes correlation and screening self-consistently through the Kohn-Sham spin-density-functional (SDF) formalism,¹¹ and can be generalized to other situations with embedded atoms.

Through the Kohn-Sham SDF formalism many-electron systems can be treated within a one-electron framework. Exchange and correlation effects are described by a functional E^{xc} of the spin density. For this functional we use the local-spin-density (LSD) approximation, as discussed in Ref. 11. Applications to atoms,¹² molecules,¹³ and solids^{12,14} suggest that for hydrogen on simple metals the LSD approximation should introduce an uncertainty in the range 0.1–0.5 eV in the binding energy, and a smaller uncertainty in energy differences like activation energies.

The idea behind our approach is to use the fact that the perturbation introduced by the adatom on the density and potential is localized because of screening, and to describe the perturbed region by a set of N functions Φ_n , localized near the

adatom and the chemisorption bond. The wave functions ψ_ν of the metal-adatom system are expanded in a basis consisting of the Φ_n 's and the unperturbed semi-infinite metal wave functions Φ_k , i.e.,

$$\psi_\nu(\vec{r}) = \sum_{n=1}^N c_n^\nu \Phi_n(\vec{r}) = \sum_k c_k^\nu \Phi_k(\vec{r}). \quad (1)$$

To make the expansion unique, the overcompleteness has to be removed by adding subsidiary conditions.¹⁵ The choice of these conditions,

$$\sum_k c_k^\nu \langle n | k \rangle = 0, \quad n = 1, \dots, N, \quad (2)$$

is one of the main points of our method. These conditions mean that $\sum_k c_k^\nu \Phi_k$ is orthogonal to all localized functions,¹⁰ i.e., that we make maximal use of the localized functions in the expansion (1) of the wave functions inside the disturbed region, while the unperturbed metal states are primarily used outside this region.

The details of our method are presented in Ref. 10. In essence, it amounts to finding the Green's function G of the one-electron equations of the Kohn-Sham SDF formalism, as an $N \times N$ matrix in the Φ_n representation. The three approximations described in Ref. 10 are used. These approximations can be systematically improved by increasing N .

As discussed above, the scheme has been applied to a model solved previously by LW,¹ i.e., an adatom nucleus of unit charge outside a semi-infinite uniform distribution of positive charge and the gas of interacting electrons.¹⁶ For the pure-metal wave functions Φ_k , a self-consistent solution of the Kohn-Sham equations by Lang and Kohn¹⁷ is exploited. The local perturbed region is assumed to be within a sphere of radius R . The local functions Φ_n have the form $F(r)Y_{lm}(\theta, \Phi)$, centered on the adatom and orthogonal in the sphere. We found that 2–3 angular and for each of them 8–10 radial functions are needed for a reasonable convergence. For $r_s = 2$ we found R about 5 Å to be suitable.

For a free-electron-like metal the effects of the lattice potential can be reintroduced through a weak pseudopotential.^{18,2} The structure-dependent effects have been calculated to lowest order by subtracting the positive background, replacing it with the pseudopotentials from the ion cores, and evaluating $\int \Delta V(\vec{r}) \Delta \rho(\vec{r}) d^3r$, where ΔV is the potential difference and $\Delta \rho$ the adatom-induced density found for $\Delta V = 0$.¹⁹ The pseudopotentials are thus screened but the screening is not self-consistent.²⁰

In summary, we have presented the first non-empirical calculation of the chemisorption energy for simple-metal substrates which includes, via a pseudopotential formalism, the ionic structure of the substrate. Our results indicate that the discrete nature of the ionic lattice plays an important role in determining the equilibrium position of the adatom. Our formalism provides a framework for describing the embedding of surface molecules and other clusters in solids. It is thus particularly encouraging that the method we have used to solve the Kohn-Sham equations for chemisorption systems yields results which are physically reasonable and which, in the case of a pure-jellium substrate, agree with those of LW.

The authors are grateful for discussions relating to this work with S. Anderson, T. B. Grimley, J. Harris, R. O. Jones, B. Kasemo, N. D. Lang, S. Lundqvist, D. M. News, J. R. Schrieffer, J. W. Wilkins, and others. Two of the authors (O. G. and H. H.) acknowledge with thanks the hospitality of the Institute of Physics, University of Aarhus.

*Supported by the Swedish Natural Science Research Council.

†Present address: Institut für Festkörperforschung der Kernforschungsanlage Jülich, D-517 Jülich, West Germany.

¹N. D. Lang and A. R. Williams, *Phys. Rev. Lett.* **34**, 531 (1975).

²We have used the potential given by N. W. Ashcroft, *Phys. Lett.* **23**, 48 (1966).

³P. E. Cade and W. M. Huo, *J. Chem. Phys.* **47**, 649 (1967).

⁴No indication of adsorption of atomic or molecular H at room temperature has been observed in ultraviolet-photoemission experiments by A. Flodström, thesis, Linköping University, 1975 (unpublished); see also, e.g., J. R. Anderson, *Structure of Metallic Crystals* (Academic, London, 1975).

⁵See, e.g., R. Gomer, in *Solid State Physics*, edited by H. Ehrenreich, F. Seitz, and D. Turnbull (Academic, New York, 1975), Vol. 30, p. 118.

⁶J. C. Slater, *Quantum Theory of Molecules and Solids* (McGraw-Hill, New York, 1975), Vol. 2.

⁷K. Ruedenberg, *Rev. Mod. Phys.* **34**, 326 (1962).

⁸It should be stressed that these spectra, $\Delta \rho(\epsilon)$, express the distribution of the energy parameters of the Kohn-Sham scheme and the relation to experimental excitation spectra is unclear.

⁹D. M. News, *Phys. Rev.* **178**, 1123 (1969).

¹⁰O. Gunnarsson and H. Hjelmberg, *Phys. Scr.* **11**, 97 (1975).

¹¹W. Kohn and L. J. Sham, *Phys. Rev.* **140**, A1133 (1965); O. Gunnarsson, B. I. Lundqvist, and S. Lund-

qvist, *Solid State Commun.* **11**, 149 (1972); O. Gunnarsson and B. I. Lundqvist, *Phys. Rev. B* **13**, 4274 (1976).

¹²B. Y. Tong and L. J. Sham, *Phys. Rev.* **144**, 1 (1966); O. Gunnarsson, B. I. Lundqvist, and J. W. Wilkins, *Phys. Rev. B* **10**, 1319 (1974).

¹³O. Gunnarsson, P. Johansson, S. Lundqvist, and B. I. Lundqvist, to be published.

¹⁴J. Janak, A. R. Williams, and V. L. Moruzzi, *Phys. Rev. B* **12**, 1257 (1975).

¹⁵T. B. Grimley, in *Dynamics of Surface Physics*, edited by F. O. Goodman (Editrice Compositori, Bologna, 1974).

¹⁶J. R. Smith, S. C. Ying, and W. Kohn, *Phys. Rev. Lett.* **30**, 610 (1973).

¹⁷N. D. Lang and W. Kohn, *Phys. Rev. B* **1**, 4555 (1970), and **3**, 1215 (1971).

¹⁸See, e.g., V. Heine, in *Solid State Physics*, edited by H. Ehrenreich, F. Seitz, and D. Turnbull (Academic, New York, 1970), Vol. 24, p. 1.

¹⁹This approach has earlier been used in Ref. 17 and by Z. D. Popovic and M. J. Stott, *Phys. Rev. Lett.* **33**, 1164 (1974).

²⁰This means that, e.g., the density dimple at the centered position is not described.

Low-Temperature Optical Investigation of the Urbach Tail in Amorphous $\text{Ge}_x\text{Te}_{1-x}$ Alloys in the Light of the Anderson Model

A. Deneuveille, A. Mini, and B. K. Chakraverty

Groupe des Transitions de Phases, Centre National de la Recherche Scientifique, 38042 Grenoble-Cédex, France

(Received 22 March 1976)

The recent Anderson model of the electronic structure of the amorphous chalcogenides predicts formation of paired localized singlet states through large electron-phonon interaction. We show that the interpretation of the absorption in the Urbach-tail region is completely consistent with modulation of band edges due to random internal electrical field associated with these bipolarons. They arise from electron transfer between Te dangling bonds, $x \leq 0.33$, or Ge dangling bonds, $x > 0.33$.

Recently, Anderson¹ has proposed a model for the electronic structure of amorphous chalcogenide semiconductors to explain the lack of EPR, of Curie paramagnetism, and of important optical absorption due to the high density ($\approx 10^{19} \text{ cm}^{-3}$) of localized states needed for pinning of the Fermi level. He has convincingly argued that the localized states must be doubly occupied electron states through strong electron-phonon interaction that overcomes the on-site Mott-Hubbard Coulomb repulsion. According to Anderson these paired states must have the following properties: (a) They do not give rise to the usual kind of conductivity as pair states need an energy higher than the single-particle mobility gap to be broken. (b) They do not give optical absorption lower than the band gap. (c) They do not respond to an external magnetic field either, since they are magnetic singlets.

Thus to all intents and purposes, these bipolaron states are "invisible." We propose in the present Letter that the study of the Urbach tail in amorphous materials can provide a direct test of the Anderson model, besides being a valuable contribution to the understanding of localized states in these chalcogenides. For the Anderson mechanism to be operative, an electron gets

transferred from one dangling bond to another—in the process, the dangling bond that is vacant becomes positively charged and the bond that receives the two electrons of opposite spin becomes negatively charged. We are thus left with a system of random positive and negative electrostatic charges, and the amorphous semiconductor resembles a highly doped compensated crystalline semiconductor (HDCCS). In this sense the Anderson model is reminiscent of the earlier models² of compensated semiconductor analogy used for amorphous semiconductors, but with the difference that now, over and above the random electrostatic fields, one will have superimposed intense local polar deformations responsible for the bipolaronic states. The number of positive and negative polar states resulting from the single-electron dangling bonds will depend strongly on the departure from the ideal tetrahedral coordination. For amorphous $\text{Ge}_x\text{Te}_{1-x}$, it seems now certain³ that this ideal tetrahedral coordination is achieved for the nominal composition GeTe_2 while Ge and Te atoms remain respectively fourfold and twofold coordinated for $x < 0.5$.⁴ On either side of $x = 0.33$, we shall expect to find an increasing number of polar "pair" states. Schematically Fig. 1 shows what one would ex-